

Analysis of Candidate Extraterrestrial Sample by Means of X-Ray Fluorescence

Ben Rasmussen

Department of Physics and Astronomy, University of Victoria

(Dated: February 8, 2024)

A candidate meteoric sample was analyzed using a variety of techniques. To test if it is from extraterrestrial origins, qualifying tests were made on the sample that included measuring its specific gravity, element composition, grain size, and qualitative investigations into the rocks properties. At a glance, the sample exhibits many of the requisite visual characteristics of a meteorite, with a fusion crust, some cracking and weathering and small metal grains on the interior with the inside much lighter than the outside. The sample is both ferromagnetic and does not leave residue behind when brought across a rough ceramic surface. In addition, the specific gravity was measured to be 3.25 ± 0.03 with grain size of $\approx 250\mu m$ with both parameters falling in the range expected of chondritic meteorites. Finally, the composition of the sample was found using X-Ray Fluorescence spectroscopy. This resulted in the presence of trace elements of Ga, Zr, Sr, and potentially Cu and Zn. More prominent features in the samples spectra were found to be Ru, Rh, and Ba. The most dominant element in the sample was found to be Fe with the additional presence of Ni. The combination of iron-nickel is required for meteorite identification. No test performed was able to disqualify the candidate as extraterrestrial, but without more detailed quantitative composition data it is hard to be absolutely conclusive of the samples origins.

I. INTRODUCTION

X-Ray Fluorescence (XRF) Spectroscopy is a powerful and relatively lightweight technique that employs knowledge of the characteristic transitions of elemental electrons to perform compositional analysis [1]. By bombarding a sample with high energy photon radiation, atoms in the material are excited to higher energy bound states. When they de-excite, a photon of specified energy is emitted. Each element will emit according to the nature of their orbitals and as such can be easily identified out of a spectrum of all emission from the sample.

Both the data acquisition and analysis using this method are relatively straightforward but the technique is limited to only detecting *elemental* components in a sample and not more complex structures [1]. The approach is non-destructive to the material making it a suitable candidate to perform analysis on fragile or intriguing samples.

In this analysis, we present a potential meteoric sample and perform a number of qualifying tests to validate its claim to extraterrestrial origin. To determine if the sample is indeed that of a meteorite, we utilized XRF spectroscopy for compositional analysis. Other discriminatory tests, or tests that can only disqualify our candidate from being a meteorite, are outlined here [2]. Among them include density and specific gravity determination, metal grain size estimates, ferromagnetism, and surface identification.

Theory:

XRF Spectroscopy

Atoms are made up of both a nucleus and surrounding bound electrons. These electrons are arranged in shells with different energy levels. Each shell is described by the principal quantum number, n . Each shell is labelled according to this number, with K corresponding to $n = 1$, L for $n = 2$, M for $n = 3$ and so on [1].

If high energy photons are incident on these bound electrons, they can excite from one shell to another absorbing the energy. Each state has corresponding energy Φ_j for the j th energy level. When the electron de-excites to lower shells, the energy emitted in the form of a photon is given by [1]:

$$E_{X-Ray} = \Phi_i - \Phi_j \quad (1)$$

Where i and j are the excited state energy and the energy of the shell the electron transitions to respectively. A transition is then labelled by the final state the electron ends up in with a further subscript denoted with either α or β for the difference between principal quantum numbers of the states involved. For example, $K_\alpha : L \rightarrow K$ and $K_\beta : M \rightarrow K$.

Each atom has distinct energies for each of these shells. We may then use these characteristic transition emissions to identify elements. The energies involved roughly follow Moseley's Law [1]:

$$\nu = a(Z - \sigma)^2 \propto Z^2 \quad (2)$$

Where ν is the emission frequency and Z is the atomic number of the element.

We may make some general notes about the limitations and features of a spectrum of emission taken from a sample using these techniques. Low Z elements have low frequencies (and energies) from equation (2) and so are difficult to find [3]. This means we are unable to test for elements like H, C, O and Si. Further, in the energy range of the detector used here, only K transitions will be picked up.

The final consideration in an XRF spectrum is due to a process involving high energy electrons in the solid sample itself. Electrons will collide with atoms in the solid, accelerating, causing photon emission proportional to the kinetic energy of the electrons. This process is called Bremsstrahlung radiation and produces a broad continuous background in the spectrum which will be proportional to the voltage of the energy source [1]. This can be seen when quantify the high energy tail of the distribution using:

$$\nu_{max} = \frac{eV}{h} \quad (3)$$

Where ν_{max} is the frequency of the high energy tail, h is Planck's constant, e is the electron charge, and V is the voltage of the X-Ray source. This effect will largely not change the presence of peaks but will rather add a considerable background to the spectrum.

Disqualifying Tests:

a. Visual Inspection:

To identify a meteorite, it must pass a number of visual tests with respect to both the exterior and interior. All meteorites are surrounded by a dark fusion crust that is considerably darker in colour to the interior. This is due to its journey through the atmosphere [2]. These crusts often flake off or break, revealing a lighter interior. They are also often accompanied by depressions on the surface, called regmaglypts, that are caused from small vortices of hot gas that locally erode the surface [2].

Most meteorites sit in two camps: iron and stony. Iron meteorites are very clearly metallic when cut open and are compositionally dominated by Iron-Nickel alloys. Of more interest to us here are stony meteorites. These can be further delineated into chondrites and achondrites. Chondrites are rocks

that have not been modified due to melting or differentiation of the source body. This means that the interiors are a mix of chondrules, or small roughly spherical molten grains of rock, and metallic grains. Achondrites consist of material that has been differentiated by the parent object and as such do not have chondrites.

To test via a visual inspection, the presence of both chondrules and metallic grains are necessary. In addition and prominent fusion crust is needed.

b. Ferromagnetism:

If a sample does not attract a permanent magnet it is very unlikely that it is a meteorite [2]. A simple test for ferromagnetism is to apply a low field magnet to the sample and see if it sticks.

c. Density and Specific Gravity:

In order to be considered to be a stony meteorite we must consider both the density and specific gravity of the sample. The density is, of course, given by:

$$\rho = \frac{m}{V} \quad (4)$$

This is a difficult quantity to measure and so we can resort to a different measure, namely the specific gravity. This is given simply by, as outlined here [4]:

$$SG = \frac{\rho_{sample}}{\rho_{H_2O}} \quad (5)$$

To actually measure this number we can use an alternate form, where D is the displacement caused due to total submergence in water of the sample:

$$SG = \frac{m_s/D}{m_D/D} \quad (6)$$

Where m_s is the mass of the sample and m_D is the mass of the displaced water by the sample.

The allowed range of specific gravity for a meteorite falls in the range [2]:

$$3.0 < SG < 3.7 \quad (7)$$

which yields a density quite a bit greater than that of terrestrial rocks.

d. The Streak Test:

Many terrestrial rocks that appear similarly to meteoric rocks are composed of iron oxides. Normal samples such as this will also pass test c) due to their density [2]. To delineate from these materials, passing the sample over a rough ceramic surface will cause oxides like hematite and magnetite to come off of the sample leaving a streak. Meteoric samples will not exhibit this property.

e. Composition:

There are many different types of meteorites with distinct formation histories and constituent parts. Excluding iron meteorites, of which this sample is not, greater than 95% of confirmed meteorites contain some combination or alloys of Iron and Nickel [2]. Depending on the metallic content, in decreasing order by mass, meteorites can be classified in either H-group, L-group, or LL-group chondrites. If a sample does not contain Iron and Nickel it is likely not extraterrestrial. To perform this test we may use XRF spectroscopy as outlined prior.

f. Grain Sizes:

The metal highlighted in test e) often manifests itself as roughly spherical grains of metal. It has been reported that for ordinary chondrites, the grain size diameter ranges from 50 to $500\mu\text{m}$ [5]. In order to quantify this, we use a very approximate approach involving 2D radial Fourier transforms. If we have a well resolved 2D image of the surface of the sample, to quantify circular features in the image as a first approximation to grain shape we may consider [6]:

$$F(\rho, \Phi) = \int_0^\infty \int_{-\pi}^{\pi} f(r, \theta) e^{-ir\rho\cos(\Phi-\theta)} r dr d\theta \quad (8)$$

In computing this quantity, we only care about the ρ dependence, contracting the function to 1 dimension. We may find the power spectrum then using:

$$S(\rho) = |F(\rho)|^2 \quad (9)$$

This can be loosely converted back into the power at a given radius using $\rho = \frac{1}{r}$. The peaks, or areas of highest spectral energy density, will then correspond to the radius at which the largest number of grains or features appear on the surface.

II. METHOD

Preparation of the Sample:

As the outer layer of the sample is different from the inner regions, it is useful to take our spectra of the internals of the rock. To do this, a diamond tipped saw courtesy of the Chemistry department glass shop was used. After splitting the sample, the surface was sanded using increasing grit sandpaper with soap and water as lubricant. The finest grit used (so far) was 2500.



FIG. 1: *Left:* Image of the outer shell of the sample. What looks like fusion crust among other features are evident. *Right:* Cross section of the image on the left polished to 2500 grit. Noticeable metallic grains are present. Radial layering is prominent but unexplained. Some *chondrules* featured.

XRF Apparatus:

To perform the X-Ray fluorescence, a number of different elements were present in the apparatus. Detection of characteristic X-Rays requires three basic things: an incident X-Ray source, a detector capable of measuring the emission from the sample, and a method to discriminate the energies of these photons. In our case, the X-Ray source used was an AmpTek Cool-X generator that utilizes a pyroelectric crystal to generate a source signal.

After hitting the sample, the emission is picked up by the Ortek PopTop Detector for low energy X-Rays. For both operational reasons and noise mitigation, this detector was cooled using liquid nitrogen to $T < 100K$. The cooling process took roughly 8 hours. The signal picked up by the detector was then sent through an additional stage of gain and

then through an AmpTek Multi-Channel Analyzer (MCA).

The variable parameters of the experiment lie within the operational voltage of the detector and the additional stage of gain. To include high energy peaks, the operational voltage was set to 50kV . This, however, caused a significant Bremsstrahlung curve that effected the data. The gain was varied for values between $10 - 250$. Doing so led to different regions of the spectra to be measured.

Calibration:

In order to begin to take data, two stages of the experimental set-up required calibration. The MCA is expected to be linearly calibrated with respect to each bin. We may then convert each of the 512 bins of the MCA to an energy value. To do this, all we need is knowledge of the energy of two bins. The most straightforward way to do this is to take a pure sample of an element (in this case Copper), measure the K_{α} and K_{β} lines at certain bins and then use the following calibration formula:

$$E - E_1 = \frac{E_2 - E_1}{b_2 - b_1} (b - b_1) \quad (10)$$

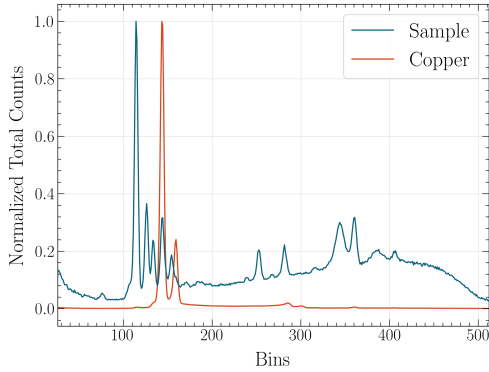


FIG. 2: Normalized Spectra of potential meteoric sample and of pure copper target for calibration. Bins of MCA corresponding to the K_{α} and K_{β} emission lines of Copper used to linearly calibrate the energy range of the detector for specific gain.

It was also noticed that the calibration here yielded strange results at high energies. This was

a function of a number of things including but not limited to the bin width of the MCA, an analysis software that calibrated incorrectly and was not used for further analysis, and a hypothesized non-linear response of the additional stage of gain. To test this, the gain was varied and the K_{α} peak of copper was traced. Fig. 3 demonstrates this showing a strong linearity with a potential loss near high gains. This would not effect our results as the final data runs were done with a gain < 175 .

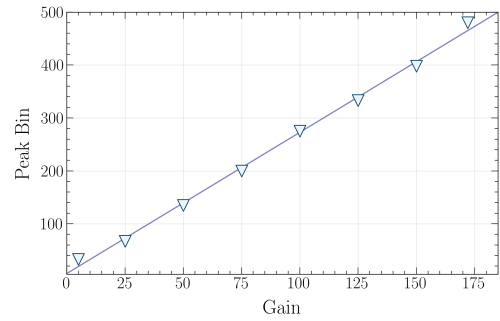


FIG. 3: Plot of the K_{α} peak of copper MCA bin as a function of the external gain. Fit is given by $Y_{bin} = (2.7 \pm 0.06)X_{gain} + (6 \pm 7)$ with $\chi^2 = 1.1$.

III. RESULTS AND ANALYSIS

As the basis of this report is to determine whether (or not) our sample is meteoric, we present our findings in the same chronology as part I. Although not conclusive, passing all 6 tests [2] means that with the technology employed here we are unable to *disqualify* the sample as extraterrestrial.

a). The first, and one of the more important tests is whether it appears as though it is a meteorite. Evidence of a fusion crust is clear, with both dark glassy surface morphology combined with light cracking on the exterior. Internally, there is evidence for some chondrules but with less than would be expected. There is, however, sufficiently large quantities of small metallic grains which are necessary for stony meteorites. These grains are small and not quite as dense as H chondrites [2]. There are more consistent with L chondrites.

b). Using a common bar magnet, the sample was tested for ferromagnetism. Even before split-

ting it in half, the magnet was moderately attracted to the sample. In cutting it in half, the magnet was strongly attracted meaning the test for ferromagnetism was positive.

c). The specific gravity was calculated using equation 6 along with mass and volume measurements made in the lab. This value was found to be $SG = 3.25 \pm 0.03$. As outlined in [2], this value falls nicely in the region $3.0 < SG < 3.7$. We may then say that the specific gravity test was conclusive.

d). One of the stranger tests highlighted here [2], the streak test was done on the rough bottom of a ceramic cup. Significant amounts of residue would disqualify the sample as being meteoric. In doing the test, barely anything was left on the ceramic regardless of the applied pressure suggesting that there is not iron oxides on the surface of the rock. We may then go on to the next test unscathed.

e). Onto the purpose of this experiment as a whole. The elemental composition of the sample was found using XRF as outlined previously. Spectra were taken for many different gains and operational voltages. For ease of comprehension, the best spectra were selected in two regions of interest (ROI). As seen in fig. 4, the sample exhibited prominent Iron emission lines. Both Nickel and Copper can also be seen in the primary ROI. The Zinc K_α line can also be seen. Of some confusion here is the lack of obvious doublets for the latter three elements. With some careful observation it appears that there are washed out K_β for Cu and Ni that are somewhat lost on a linear scale. The Zinc doublet partner is outside of the ROI. It is then fairly reasonable to conclude the presence of Cu, Zn, and Ni in the sample with a considerable relative amount of Iron. Of note here is the relative quantity of Fe and Ni. As mentioned previously, the ratio of Iron to Nickel plays a role in the categorization of meteorites. It is likely that this is an iron dominated sample when compared to Nickel. Without more detailed knowledge of the set up and the fundamental parameters of the material (see Appendix A) we cannot make conclusions about the mass compositions, as we will be further challenged about in the succeeding paragraph.

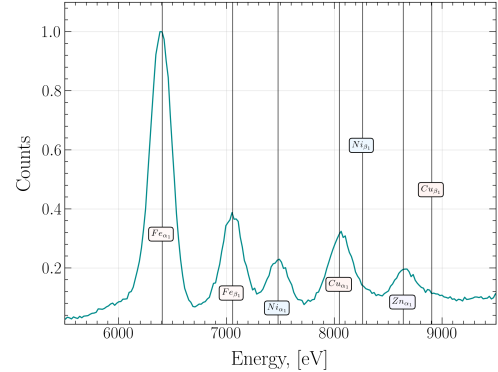


FIG. 4: Normalized candidate spectra in primary region of interest with a gain of 40. Fe , Ni , Cu , and Zn characteristic emission energies overlaid

To analyze more exotic materials, the entire energy range is shown in fig. 5 on a different data run with a gain of 40. The first very prominent feature of the spectrum is the large Bremsstrahlung curve that traces energies after $E \approx 20000$. This is due to the large operational voltage needed to observe the high energy region.

From left to right, we will attempt to untangle the plot in fig. 5. As with the primary ROI, iron and nickel are both present with Fe dominating the region. A lack of copper and zinc peaks is a notable feature when compared to fig. 4. Gallium, Strontium, and Zirconium fill in the bulk of the lower-middle energy region. These are all reasonably expected constituents when following [7] with Zirconium as the rarest to be found in meteorites.

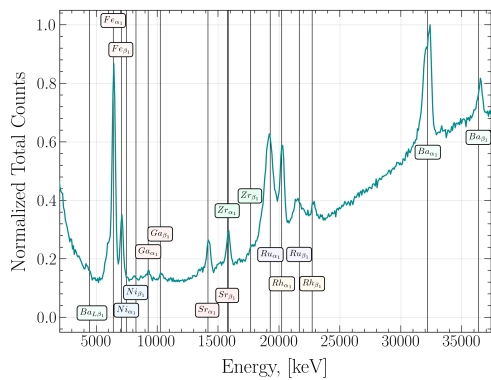


FIG. 5: Normalized candidate spectra for the entire energy range with a gain of 40. All identified elemental emission energies overlaid. Noticeable doublets are found for almost all potential constituents.

In the center of the plot we find a somewhat strange set of features. The energy of the peaks here correspond to Ruthenium and Rhodium, two unexpected contributors. It is not unheard of to find either element as found in [7] with Rhodium being quite rare when compared to even Ruthenium. What makes these peaks particularly interesting is that both the K_α and K_β peaks can be found as a pair with reasonable accuracy. Unless the calibration was not done properly, there is both Ruthenium and Rhodium in the sample. One thing to note is that it has been reported that a marked Ruthenium abundance in a meteorite seems to inversely relate to the Nickel abundance [8] so if our candidate is indeed meteoric that would somewhat explain a lower nickel content.

Finally moving to the high energy region, we find that there is a considerable Barium signature. This, too, is not incredibly surprising but still odd that the signal is so strong. In Barium's favour is the presence of a convenient L_α line in the low energy regime. An attempt to better quantify each elemental contribution can be found in Appendix A.

All found elements have historically been found in meteorites. The presence of all three of Rhodium, Ruthenium, and Barium with considerable relative strength is definitely of interest but does not disqualify the sample from our goal. In order to make a conclusion to this test, we have identified both Iron and Nickel, two of the primary constituents and re-

quired elements of meteorites. Once again we are unable to disqualify the sample as being not from Earth.

f). Our final test pertains to the grain sizes of the sample. A high resolution image of the surface of the rock was taken and displayed using a contrasting colour-map to show the metal grains explicitly. This can be seen in fig. 6.

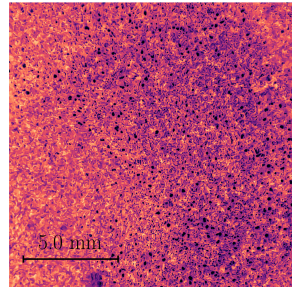


FIG. 6: High resolution image of surface shown in fig. 1 using contrast colour map to highlight grains. Length scale overlaid.

To quantify the size of the grains, assuming circular granularity, we implemented a discrete analog to equation (8). This was then converted to a power spectra using equation (9) in units of radius. This power spectrum can be seen in fig. 7. Obvious peaks in power are labelled on the image. It is clear from the image, that the dominant feature size of objects in the image, in descending order, are $R = 0.25\text{mm}$, $R = 0.69\text{mm}$, and $R = 1.14\text{mm}$. The first peak contains the majority of the power of the image and so we can say that the grain sizes, to first order and assuming circular symmetry, are $R \approx 0.25\text{mm}$.

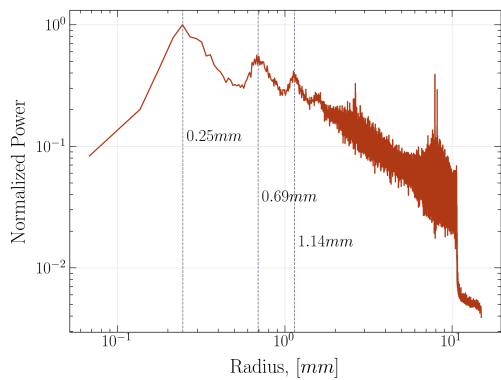


FIG. 7: Power spectrum of the radial Fourier transform of fig. 6 converted to units of [mm]. Peaks of significant contributions to the image are highlighted with dashed vertical lines.

As mentioned in section I., the range for ordinary chondrite meteorites for their metal grain sizes is:

$$50\mu m < R < 500\mu m$$

Converting our value to μm gives $R_{sample} \approx 250\mu m$. Using this somewhat hand-wavy approach, we obtain a grain size that falls right in the middle of the allowable range. We are once again unable to adequately disqualify our sample as being extraterrestrial and we may say that this test is also positive.

IV. DISCUSSION

In this paper, a number of tests were performed on a potential meteoric candidate. By visual inspection, there exists what appears to be a fusion crust, with the exterior being a much darker colour than the interior and some visible cracking on the surface. As for the internals, the presence of metal grains is definitive. Some chondrules can be seen but less than one would expect. The size and distribution suggest that the sample is more metal-poor than the H-type chondrites seen here [2]. We may then consider that the object is of the L-type variety if it is a meteorite.

The sample was also found to be clearly ferromagnetic. In addition, the specific gravity was calculated to be $SG = 3.25 \pm 0.03$. This falls well within the range expected of meteorites. Uncertainty here

was supplied purely from the standard uncertainty of measurement for the procedure. The sample was also confirmed to not be made up of iron-oxides by running it against a rough ceramic surface, passing another test.

The composition of the meteorite was found using an XRF method. This resulted in elemental confirmation of Ga, Ru, and Rh, with trace amounts of Ga, Zr, and Sr. Potential peaks of both Cu and Zn were also found. Dominating the spectra was Fe which is expected of a meteorite. In addition, Ni signatures were confirmed. These last two elements are the primary indicator of whether a sample is meteoric or not.

The primary difficulty involved in this test was proper calibration. As the energy differences between separate elements can be small, even the 512 bin resolution of the energy range has an effect on the overall calibration. To mitigate problems with the calibration, it was done by-hand for many different samples with varying gain and supply voltage. These data runs all resulted in similar compositional conclusions. Further complications arise when we considered a potential non-linearity in the gain. It was found, however, that in our operating regime this had little to no effect on the overall calibration.

The final test performed was a test on the grain sizes of the sample. Using fourier analysis, a power spectrum of the radial size of features in the image was produced. The dominant peak in this spectrum fell at a radius of $0.25mm$ which lies well within the accepted range of metallic grain sizes for ordinary chondrites.

V. CONCLUSION

To validate the the claim of our samples extraterrestrial origin, standard tests were performed. Visually, the sample likely falls in the L-type chondrite taxonomy due to the stony nature of the sample and the presence of low but prominent small metallic grains. All six of the tests were negative tests in nature and so it is difficult to truly confirm if the sample is meteoric. That being said, not one of the six tests performed yielded a negative result. We are then unable to conclude that the sample is *not* meteoric. It is the opinion of this author that the sample is indeed a meteorite.

VI. ACKNOWLEDGEMENTS

The sample used in this report was graciously provided by Dr. Jon Willis. For his I thank him. Further thanks is extended to Adam in the chemistry glass shop who both cut the sample with a diamond saw and provided the tools necessary for polishing.

-
- [1] J. Robinson, E. Frame, and G. Frame II, *Undergraduate Instrumental Analysis* (7th ed.). (CRC Press, 2024).
 - [2] R. L. Korotev, *Some Meteorite Information*, Tech. Rep. (2024) [Accessed: 5-February 2024].
 - [3] A. S. D. Library, *Interpretation of XRF Spectra*, Tech. Rep. (2023) [Accessed: 5-February 2024].
 - [4] E. R. Gordon, *Density and Specific Gravity*, Tech. Rep. (2023) [Accessed: 5-February 2024].
 - [5] A. J. Campbell and M. Humayun, *Geochimica et Cosmochimica Acta* **67**, 2481 (2003).
 - [6] N. Baddour, *Advances in Imaging and Electron Physics*, **165**, 2 (2011).
 - [7] H. E. Suess, “Astronomy and astrophysics · 3.4 stars: Datasheet from landolt-börnstein - group vi astronomy and astrophysics · volume 1: “astronomy and astrophysics” in springermaterials (https://doi.org/10.1007/10201941_16),”.
 - [8] T. Hara and E. B. Sandell, *Geochimica et Cosmochimica Acta* **21**, 145 (1960).
 - [9] V. Solé, E. Papillon, M. Cotte, P. Walter, and J. Susini, *Spectrochimica Acta Part B: Atomic Spectroscopy* **62**, 63 (2007).
 - [10] J. B. Kortright and A. C. Thompson, *X-Ray Properties of the Elements*, Tech. Rep. (2000) [Accessed: 5-February 2024].

APPENDIX A: An Attempt at Quantitative Analysis

The last significant piece of the puzzle for this analysis is to perform a *quantitative* analysis of the sample composition. This has proven to be considerably difficult and likely outside of the scope of a paper such as this. Intimate knowledge of the detector environment and morphology is needed as the output spectra is dependent on the incident angle of the X-rays as well as the geometry and composition of all elements of the apparatus.

To complete a proper analysis of the sample and be more certain in the conclusions drawn in this lab, constituent mass fractions should be found. In exploring this avenue, a number of synthetic spectra were generated for the purpose of both qualitative and quantitative analysis. These were created using the software package PYMCA found here [9].

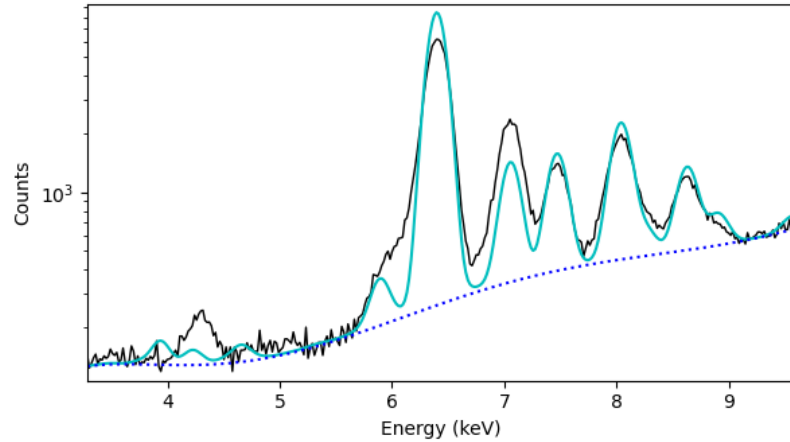


FIG. 8: Generated synthetic spectrum using the software PYMCA for similar ROI as fig. 4. Background generated using a Pseudo-Voigt method with exponential polynomial basis functions. Synthetic curve made up of all constituent parts found qualitatively in fig. 4 with the addition of Manganese.

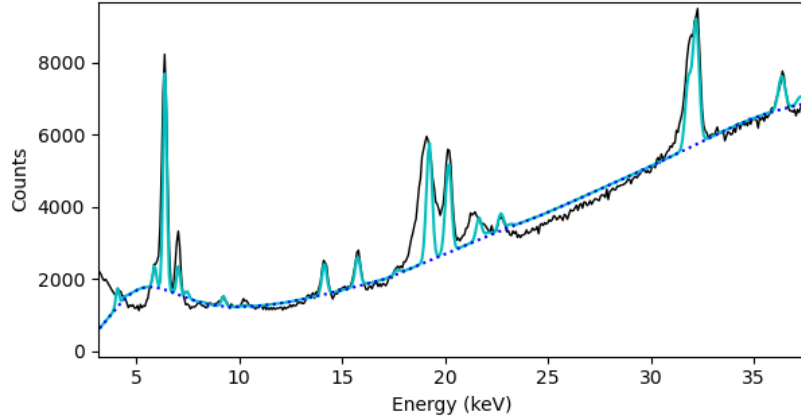


FIG. 9: Generated synthetic spectrum using the software PYMCA for entire spectral range. Background generated using a Pseudo-Voigt method with exponential polynomial basis functions. Synthetic curve made up of all constituent parts found qualitatively in fig. 5 with the addition of Manganese and Scandium.

As seen in fig. 8 and fig. 9, well-fitted spectra were generated for ROIs similar to fig. 4, 5. The black, noisy line corresponds to the data obtained using the XRF set-up with the cyan curve being as the spectrum computed by PYMCA. As we have considerable Bremsstrahlung from the sample for high input energies (50 kV), a background was estimated using the same program which is drawn in blue dashed lines.

In doing this analysis, it became clear that the initial findings were incomplete. All synthetic spectra confirmed the additional existence of Manganese (fig. 8) and Manganese and Scandium (fig. 9). There are clearly some over- and underestimates of the spectra but the general form of the data is well described by the synthetic spectra with Bremsstrahlung background included.

We may compute a somewhat incomplete relative contribution to the fit to see which elements are significant. To do so, we define a metric as follows. Since we have no prior knowledge of the composition of the sample, we calculate a *relative to Iron* coefficient as Iron is the most prevalent element:

$$R_{Fe} = \frac{\mu_X}{\mu_{Fe}}$$

Where μ_X is the elemental contribution to the total fit *area* and μ_{Fe} is the Iron contribution.

Element	μ_X	R_{Fe}
Fe	22632	1
Mn	2698.5	0.12
Sc	2422.6	0.11
Ga	499.43	0.02
Ni	15718	0.69
Sr	4770.8	0.21
Zr	4193	0.19
Ru	18240	0.81
Rh	18611	0.82
Ba	18713	0.83

TABLE I: Relative contributions to the total fit area found in fig. 9. Can roughly be grouped into three camps. *Trace*: Manganese, Scandium, and Gallium are small compared to the total iron. *Moderate*: Strontium and Zirconium contribute much less than iron but are significant. *Bulk*: Barium, Ruthenium, Rhodium, and Nickel are all comparable to Iron in their contributions.

APPENDIX B: Energies of Identified Elements

Element	$K\alpha_1$	$K\alpha_2$	$K\beta_1$
21 Sc	4,090.6	4,086.1	4,460.5
25 Mn	5,898.75	5,887.65	6,490.45
26 Fe	6,403.84	6,390.84	7,057.98
28 Ni	7,478.15	7,460.89	8,264.66
29 Cu	8,047.78	8,027.83	8,905.29
30 Zn	8,638.86	8,615.78	9,572.0
31 Ga	9,251.74	9,224.82	10,264.2
38 Sr	14,165	14,097.9	15,835.7
40 Zr	15,775.1	15,690.9	17,667.8
44 Ru	19,279.2	19,150.4	21,656.8
45 Rh	20,216.1	20,073.7	22,723.6
56 Ba	32,193.6	31,817.1	36,378.2

TABLE II: Characteristic emission energies for all of the found elements in the sample using the data found here [10]. In units of keV .